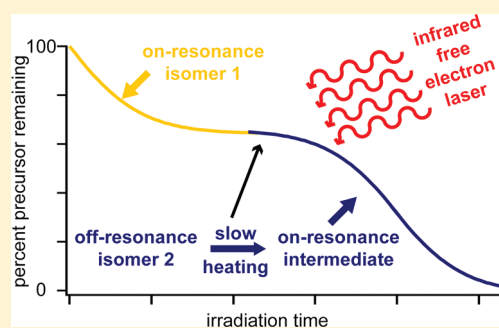


# Isomer Population Analysis of Gaseous Ions From Infrared Multiple Photon Dissociation Kinetics

James S. Prell,<sup>†</sup> Terrence M. Chang,<sup>†</sup> Jeffrey A. Biles,<sup>†</sup> Giel Berden,<sup>‡,§</sup> Jos Oomens,<sup>‡,§</sup> and Evan R. Williams<sup>\*,†</sup><sup>†</sup>Department of Chemistry, University of California, Berkeley, California 94720-1460, United States<sup>‡</sup>FOM Institute for Plasma Physics Rijnhuizen, Edisonbaan 14, 3439 MN Nieuwegein, The Netherlands<sup>§</sup>University of Amsterdam, Science Park 904, 1098XH Amsterdam, The Netherlands

**ABSTRACT:** Infrared multiple photon dissociation (IRMPD) kinetics measured with tunable laser radiation from a free electron laser (FEL) are used to probe the relative populations of and interconversions between energetically competitive isomers of gas-phase ions at 298 K. On-resonance IRMPD kinetics of monoisomeric benzoate anion and anilinium (protonated aniline) are measured to determine the extent of overlap of the laser beam with the precursor ion population (~93%). IRMPD kinetics indicating different photodissociation behavior for different isomers obtained at isomer-specific resonances are used to determine relative populations of salt bridge and charge-solvated isomers for ArgGly·Na<sup>+</sup>, Ser·Cs<sup>+</sup>, and Arg·Na<sup>+</sup>. These values and Gibbs free energy differences obtained from them for thermal precursor populations are compared to values reported using other, less direct population probes. Rapid interconversion of two charge-solvated isomers occurs for ArgGly·Li<sup>+</sup>, precluding population analysis for this ion. ArgGly·Na<sup>+</sup>, ArgGly·Li<sup>+</sup>, and Arg·Na<sup>+</sup> exhibit IRMPD induction periods lasting many seconds for some isomers at the laser photon energies and power used, indicating that IRMPD relative spectral intensities are time-dependent for these ions and that the relative band intensities in IRMPD spectra measured with short irradiation times may not provide meaningful information about relative isomer populations. These results constitute the first direct probe of ion isomer populations using IRMPD kinetics obtained with a FEL and illustrate a number of caveats in interpreting IRMPD spectra measured with just a single irradiation time. These results also indicate that more complete overlap of the laser beam with the ions will be highly advantageous in future instrument designs for IRMPD kinetics and spectroscopy experiments.



## INTRODUCTION

Infrared multiple photon dissociation (IRMPD) and the very similar infrared photodissociation (IRPD) spectroscopies, in which photofragmentation of gas-phase ions or molecules induced by infrared laser radiation is measured as a function of photon energy, have become widely used methods for ion structure elucidation in the past decade.<sup>1,2</sup> For small ions with high initial internal energies or with low dissociation barriers, fragmentation can be increased substantially upon absorption of even a single photon, making it possible to perform these experiments using a mass spectrometer coupled to a low-power table-top laser system.<sup>1,3–17</sup> For ions with low initial internal energies or high dissociation barriers, absorption of multiple infrared photons is often required to produce measurable fragmentation, making higher laser power, such as that readily available with free electron lasers (FELs)<sup>1,2,18,19</sup> including CLIO (Laser Infrarouge d'Orsay)<sup>18</sup> and FELIX (Free Electron Laser for Infrared eXperiments),<sup>19</sup> advantageous. The IR(M)PD spectra resulting from these experiments provide information about vibrational resonances of the ion of interest, and under some conditions,<sup>20</sup> these spectra can be very similar to IR absorption spectra. Because the vibrational spectra of many ions can be highly sensitive to structural differences, including hydrogen

bonding, neutral versus salt-bridge structures, and cation or anion coordination, these methods are applicable to a wide range of ions.

The initial ion population in IR(M)PD spectroscopy experiments can consist of a thermal distribution of structures, or some higher-energy structures may be kinetically trapped, depending on how the ions are formed. Evidence for kinetic trapping of both small<sup>21,22</sup> and large ions<sup>23–25</sup> formed by electrospray ionization has been reported. For experiments where a thermal population of ions is formed, measuring the relative isomer populations can be especially valuable because it exposes the thermally accessible conformational landscape and indicates that the isomer families lie within a few *kT* of each other. Accurate measurement of these competitive isomer populations (and, hence, thermodynamic information such as relative Gibbs free energies, enthalpies, and entropies) also provide benchmarks that are desirable for improving computational chemistry.

Matching measured spectra to linear superpositions of calculated harmonic absorption spectra or IR(M)PD spectra of “model”

Received: January 14, 2011

Revised: February 24, 2011

Published: March 16, 2011

ions or molecules of known structure have been used to obtain estimates of isomer populations.<sup>5,26,27</sup> As has been demonstrated for many ions, calculated relative band intensities can be poor predictors of experimental intensities,<sup>5,27–33</sup> resulting in significant uncertainty with the former method of estimating relative isomer populations. In addition, many IRMPD spectra are reported as a photodissociation yield that does not vary linearly with absorption.<sup>20</sup> The use of model ions can also be problematic due to the dependence of IR(M)PD band intensities on ion dissociation energy, which can differ substantially between various isomers. If photodissociation kinetics are biexponential due to the presence of two spectroscopically distinguishable isomers, as has been demonstrated recently for some hydrated, protonated amino acids,<sup>34,35</sup> relative IR(M)PD spectral band intensities will depend on irradiation time, and spectra measured at just a single irradiation time will not provide meaningful information about relative isomer populations.

Several experimental gas-phase techniques have been introduced that have begun to address some of these challenges. Isomer selection of cold, argon-tagged ions and subsequent measurement of single-isomer infrared photodissociation spectra has been demonstrated,<sup>36,37</sup> and measurement of isomerization barriers in neutral molecules has been achieved.<sup>38,39</sup> IR/UV ion-dip spectroscopy, in which changes in isomer-specific ultraviolet laser-induced photodissociation are measured after irradiation with tunable infrared radiation, has also been used to obtain isomer-specific vibrational spectra of ions.<sup>40,41</sup> Isomer populations are not typically obtained using this method in part owing to the difficulties of quantifying isomer populations based on band intensities alone. We recently showed that IRPD kinetics measured using a simple table-top laser system coupled to a Fourier transform ion cyclotron resonance (FT/ICR) mass spectrometer can be used to probe the relative populations of ion isomers at photon energies resonant with only one isomer population.<sup>34,35</sup> For ions with two spectroscopically distinguishable ion populations, resonant and nonresonant ion populations dissociate with different first-order rate constants, resulting in biexponential kinetics that can be fitted to obtain relative isomer populations from the pre-exponential factors. This method is analogous to the simultaneous acquisition of individual dissociation mass spectra of isomers from blackbody infrared radiative dissociation kinetics demonstrated previously.<sup>42</sup> When this method is used, the preferences for water binding to the four acidic proton sites in protonated phenylalanine were measured, and Gibbs free energy differences for binding to these sites were obtained.<sup>34</sup> This technique was also used to measure the temperature-dependence of water molecule binding to the positively charged N-terminal ammonium group versus neutral carboxylic acid group in protonated proline, where it was thereby determined that entropy drives an attached water molecule from the C-terminus to the N-terminus with increasing temperature.<sup>35</sup> This technique should be widely applicable for a variety of ions with isomer populations that do not interconvert on time scales faster than photodissociation.

Here we report IRMPD kinetics obtained using FELIX for several ions<sup>26–28</sup> for which previously published IRMPD spectra using this FEL indicate multiple spectroscopically distinguishable isomer populations at 298 K. These results show that this method for directly measuring relative isomer populations and probing isomerization dynamics can be extended to IRMPD kinetics measured using a FEL. These results also illustrate some of the limitations of interpreting IR(M)PD spectra acquired using just a

single irradiation time, as has been done in most previous gas-phase ion spectroscopy applications in which FELs are used.

## EXPERIMENTAL METHODS

All data were obtained using a 4.7 T Fourier-transform ion cyclotron resonance mass spectrometer.<sup>19</sup> Samples were prepared from Arg (Fluka, Buchs, Switzerland), ArgGly (Bachem, Weil am Rhein, Germany; obtained as a hydrochloride salt), Ser (Aldrich), aniline, and benzoic acid as a 2–3 mM 4/1 methanol/water solution. LiCl, NaCl, KCl, or CsCl (1–3 mM) were added to the Arg, Ser, and ArgGly solutions. Electrospray ionization was used to produce the ions from solution with a flow rate of  $\sim 10 \mu\text{L}/\text{min}$ . Precursor ions were isolated with stored waveform inverse Fourier-transforms prior to irradiation. The pressure measured above a turbomolecular pump that is  $\sim 1 \text{ m}$  from the ion cell is  $\sim 2\text{--}3 \times 10^{-8} \text{ Torr}$ .

A free electron laser (FELIX) operating at 5 Hz was used to induce dissociation of the precursor ions. A detailed description of the instrument and the FEL is given elsewhere.<sup>19,43</sup> The laser energy entering the mass spectrometer was 18–25 mJ per 6  $\mu\text{s}$  macropulse, and the laser intensity was attenuated by 50% when irradiating Ser·Cs<sup>+</sup> due to its especially fast on-resonance photodissociation, but the laser was not attenuated when dissociating the other samples. The ions were irradiated at photon energies corresponding to photodissociation maxima found by scanning the laser photon energy near the spectral band of interest. At least 10 different irradiation times were used for each ion, including at least one data point where >90% depletion of the precursor ion was observed. Where applicable, mono- and biexponential fits were obtained using Igor v. 4.07 (Wavemetrics, Portland, OR, U.S.A.).

## RESULTS AND DISCUSSION

**Overlap of Laser Light with the Trapped Ions.** In an ideal IRMPD kinetics experiment, there should be complete overlap of the laser light with the ion population so that complete dissociation of the precursor population is possible and kinetics are first-order when only a single isomer population is present. The irradiation geometry and ion cell design can affect the fraction of ions that strongly overlap with the laser radiation, and a high degree of overlap is advantageous for simplifying interpretation of photodissociation kinetics and IRMPD spectral data. Nearly complete overlap is possible using an irradiation geometry where the laser beam is on axis with the ion cell, and >96% photodissociation with first-order, monoexponential kinetics has been demonstrated in spectroscopy experiments.<sup>35</sup>

To establish what fraction of the ion population overlaps the laser beam in the FT/ICR ion cell coupled to FELIX, where an off-axis, multipass geometry is used,<sup>1</sup> benzoate anion and anilinium (protonated aniline) were photodissociated on resonance. These ions are monoisomeric at room temperature, and IRMPD should result in first-order, monoexponential photodissociation. Photodissociation kinetics of these two ions at the carboxylate antisymmetric stretch ( $1630 \text{ cm}^{-1}$ ) for benzoate and NH umbrella motion ( $1447 \text{ cm}^{-1}$ ) for anilinium are shown in Figure 1, and product ions for these and all other ions investigated are listed in Table 1. Irradiation of benzoate induces loss of CO<sub>2</sub> to produce phenide anion ( $m/z$  77), the abundance of which increases until  $\sim 12 \text{ s}$  irradiation time. At longer irradiation times, the abundance of phenide anion decreases and methoxide

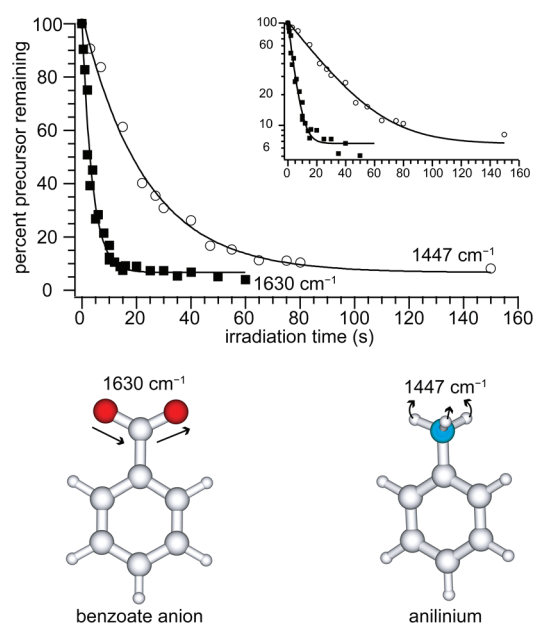


**Figure 1.** IRMPD kinetics for benzoate anion (filled squares) and anilinium (open circles) at 1630 and 1447  $\text{cm}^{-1}$ , respectively, with monoexponential fits (lines). The same data with a logarithmic  $y$ -axis are inset to make the fraction of nondissociable ions clearer. Arrows in representative structures indicate the vibrational modes excited at photon energies used.

( $m/z$  31) is observed. Background neutral methanol originating from the electrospray plume is present in the ion cell, and these results are consistent with formation of methoxide by proton transfer from neutral methanol inside the ion trap to phenide anion, which is significantly more basic than methoxide. Benzoate radical has an electron affinity of  $\sim 3.75$  eV at room temperature,<sup>44</sup> thus, spontaneous neutralization of benzoate anion by ejection of an electron is unlikely to occur in these experiments unless the ion has absorbed laser radiation and therefore constitutes one photodissociation pathway for this precursor. Methoxide is significantly more basic than the benzoate anion in the gas phase,<sup>44</sup> thus, neutralization of benzoate by proton transfer from neutral methanol is also unlikely. Because the products of laser-induced electron ejection of benzoate anion cannot be detected directly in these experiments, the extent of laser-induced dissociation of this precursor ion was calculated as the precursor abundance after irradiation divided by the precursor abundance measured with 0 s irradiation in order to account for this reaction as well as the phenide and methoxide ion formation described above. Anilinium dissociates primarily by loss of  $\text{NH}_3$ , but minor products corresponding to the aromatic ion series at  $m/z = 66, 65, 51,$  and  $39$  were also observed. For this and all other ions, the extent of dissociation was determined from the precursor abundance and the sum of the abundances of all fragment ions.

No induction period is observed for either benzoate anion or anilinium, indicating that these ions heat quickly and dissociate promptly at the photon energies and laser power used. The kinetics for both ions are first-order, monoexponential to  $\sim 93\%$  depletion of the precursor ion, indicating that  $\sim 7\%$  of the ion population overlaps poorly with the laser beam. For anilinium, deviation from monoexponential kinetics occurs at irradiation times longer than  $\sim 80$  s. This deviation may be due to an increase in magnetron motion with time that results in reduced

**Table 1.** Photodissociation Product Ions Detected for Benzoate Anion, Anilinium,  $\text{ArgGly}\cdot\text{Na}^+$ ,  $\text{ArgGly}\cdot\text{Li}^+$ ,  $\text{Arg}\cdot\text{Na}^+$ , and  $\text{Ser}\cdot\text{Cs}^+$

precursor ion	product ion $m/z$	assignment
benzoate anion ( $m/z$ 121)	77	$\text{C}_6\text{H}_5^-$
	31	methoxide
	77	$-\text{NH}_3$
	66, 65, 51, 39	aromatic ion series
anilinium ( $m/z$ 94)	236	$-\text{H}_2\text{O}$
	194	loss of 60 Da <sup>a</sup>
	179	loss of glycine
	137	(unassigned)
$\text{ArgGly}\cdot\text{Na}^+$ ( $m/z$ 254)	23	$\text{Na}^+$
	220	$-\text{H}_2\text{O}$
	178	loss of 60 Da <sup>a</sup>
	163	loss of glycine
$\text{ArgGly}\cdot\text{Li}^+$ ( $m/z$ 238)	135, 121, 118	(unassigned)
	133	$\text{Cs}^+$
	180	$-\text{NH}_3$
	179	$-\text{H}_2\text{O}$
$\text{Arg}\cdot\text{Na}^+$ ( $m/z$ 197)	137	loss of 60 Da <sup>a</sup>
	23	$\text{Na}^+$

<sup>a</sup> Fragmentation products corresponding to the loss of 60 Da have been reported in collisionally induced dissociation mass spectra for Arg-containing ions and are discussed elsewhere (Forbes, M. W.; Jockusch, R. A.; Young, A. B.; Harrison, A. G. *J. Am. Soc. Mass Spectrom.* **2007**, *18*, 1959–1966).

overlap of the ion population with the laser beam. Precursor ions with similar  $m/z$  are expected to have similar overlap with the laser beam when using similar instrumental conditions, and this value of 93% is used in the analysis of the data described below.

**Separating Ion Populations with Slow Isomer Interconversion:  $\text{ArgGly}\cdot\text{Na}^+$ .**  $\text{ArgGly}\cdot\text{Na}^+$  adopts a mixture of salt-bridge (SB) and charge-solvated (CS) structures at 298 K.<sup>27</sup> In the SB structure, the C-terminus of ArgGly is deprotonated and the arginine side chain is protonated. In the CS structure, the C-terminus and side chain are formally neutral. These populations are distinguished spectroscopically by the presence of both a strong C-terminal hydroxyl in-plane bend at 1149  $\text{cm}^{-1}$  and C-terminal carbonyl stretch at 1748  $\text{cm}^{-1}$  for the CS structures, whereas strong bands are absent in these regions for the SB structure.<sup>27</sup> Photodissociation kinetics of  $\text{ArgGly}\cdot\text{Na}^+$  at these two photon energies are shown in Figure 2. Irradiation at these two frequencies resonantly excites CS isomers, resulting in prompt dissociation, whereas the remaining SB population dissociates much more slowly due to off-resonance absorption or slow interconversion to CS isomers.

A direct measurement of the CS isomer population without multiexponential fitting of these kinetic data is possible due to the presence of an inflection point that occurs when the photodissociation rate decreases substantially before increasing again at longer irradiation times. This inflection point at  $\sim 63$  (1149  $\text{cm}^{-1}$ ) and  $\sim 80\%$  (1748  $\text{cm}^{-1}$ ) depletion of the precursor ion reflects the time at which nearly complete dissociation of the initial CS population has occurred and the slow-heating induction period for dissociation of the SB population has come to an end. Because up to  $\sim 7\%$  of the ion population has poor overlap with the laser beam, these results indicate that  $\sim 63$ – $86\%$  (63/100 to 80/93)

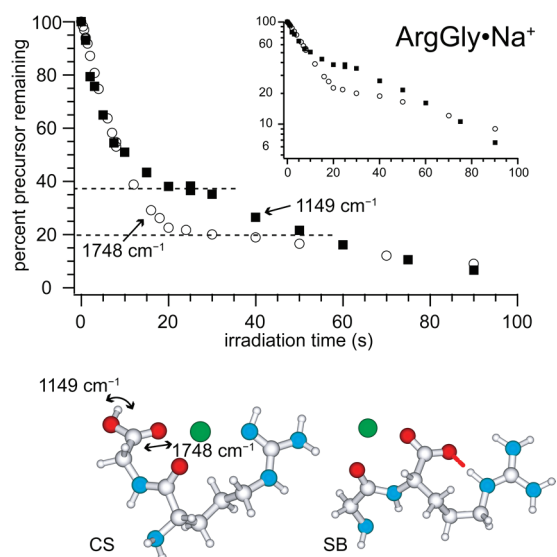


**Figure 2.** IRMPD kinetics for ArgGly·Na<sup>+</sup> at 1149 (filled squares) and 1748 cm<sup>-1</sup> (open circles), with dashed lines indicating the *y*-value of the inflection point in the 1149 (upper) and 1748 cm<sup>-1</sup> (lower) data. The same data with a logarithmic *y*-axis are inset to make relative instantaneous first-order rate constants clearer. Arrows in the representative CS structure indicate the vibrational modes excited at the photon energies used.

of the precursor adopts a CS structure and the remaining ~14–37% adopts a SB structure. These populations are somewhat different from those (~40% CS and ~60% SB) estimated by fitting the IRMPD spectrum of ArgGly·Na<sup>+</sup> with superimposed, normalized spectra of ArgGly·Li<sup>+</sup> and ArgGly·K<sup>+</sup> as models for the spectra of pure CS and SB populations, respectively.<sup>27</sup> These results also indicate that relative IRMPD band intensities for ArgGly·Na<sup>+</sup> acquired using a single irradiation time are time-dependent, thus, relative populations obtained from superimposing model spectra may not be unique and may depend on the choice of irradiation time. The discrepancy between the populations derived from IRMPD kinetics versus model spectrum superposition illustrates the potential inaccuracy of the latter method.

Loss of H<sub>2</sub>O is the dominant dissociation channel at all irradiation times and can occur from a SB structure via an ion intermediate with a CS structure.<sup>27</sup> The H<sub>2</sub>O loss channel and the return to faster dissociation at longer irradiation times are consistent with slow interconversion of the weakly resonant SB population to a strongly resonant CS isomer(s), as opposed to more direct, off-resonant fragmentation of SB structures. This distinction highlights the utility of measuring photodissociation as a function of time, because such dynamical information can be obscured in IRMPD experiments when just a single irradiation time is used.

**Rapid Isomer Interconversion: ArgGly·Li<sup>+</sup>.** Previous experiments indicate that ArgGly·Li<sup>+</sup> adopts a mixture of two spectroscopically distinguishable CS isomer families with a C-terminal carbonyl stretch band at either 1739 or 1776 cm<sup>-1</sup>.<sup>27</sup> The former population was identified as isomers with an *endo* carboxylic acid group, whereas the latter population has an *exo* carboxylic acid group. Irradiation at these two frequencies results in the photodissociation kinetics shown in Figure 3. The kinetics at the lower photon energy are first-order, monoexponential to over 90% depletion of the precursor. Kinetics at the higher photon energy exhibit an induction period<sup>20,45–47</sup> that lasts until

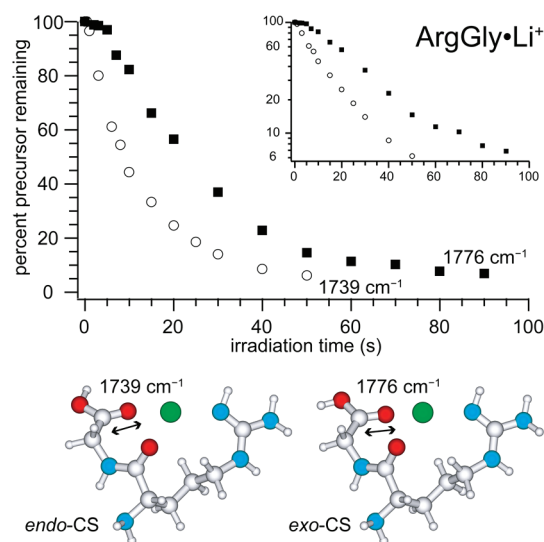


**Figure 3.** IRMPD kinetics for ArgGly·Li<sup>+</sup> at 1739 (open circles) and 1776 cm<sup>-1</sup> (filled squares). The same data with a logarithmic *y*-axis are inset to make the first-order, monoexponential kinetic behavior and induction period (for the 1776 cm<sup>-1</sup> data) clearer. Arrows in representative structures indicate the vibrational modes excited at photon energies used.

~5 s, after which first-order, monoexponential kinetics to ~90% depletion of the precursor is observed. The induction period is due to slow heating of the ion population until a steady state dissociating population is achieved.<sup>20,45–47</sup> The first-order rate constant obtained from fitting the 1739 cm<sup>-1</sup> data is ~1.6 times as fast as that for the 1776 cm<sup>-1</sup> after the induction period. Thus, the lack of an induction period at the lower photon energy could be the result of more rapid absorption of energy at 1739 cm<sup>-1</sup> and a significantly higher barrier to dissociation for the population resonant at 1776 cm<sup>-1</sup>. The first-order, monoexponential kinetics measured at both laser photon energies indicate that the two CS isomer populations can rapidly interconvert on a time-scale faster than photodissociation. It is consequently not possible to determine the relative isomer populations from these kinetic data.

These results are especially significant in light of “missing” bands and lowest-energy population assignments reported in the IR(M)PD spectroscopy literature. The presence or absence of an ion isomer family is often reported in the IR(M)PD spectroscopy literature based on the presence or absence of spectroscopically unique bands associated with that isomer family.<sup>8,21,26–29,31–33,48–65</sup> For ions with significant photodissociation induction periods at such bands, irradiation for times shorter than the induction period will lead to the erroneous conclusion that the relevant isomer is not present, and failure to account for the induction period properly will lead to IRMPD spectra where relative peak intensities can vary substantially as a function of irradiation time. For example, the ratio of the “apparent” first-order rate constants,  $k_{\text{app}}$ , corresponding to the band maxima at 1739 and 1776 cm<sup>-1</sup>, with  $k_{\text{app}}$  defined as

$$k_{\text{app}} \equiv \frac{-1}{t_{\text{irr}}} \times \ln \left( \frac{[\text{precursor}]}{[\text{precursor}] + \sum [\text{products}]} \right)$$

would be >14:1 at  $t_{\text{irr}} = 3$  s, whereas if the induction period is properly taken into account, this ratio is ~1.6:1. Thus, the band at 1739 cm<sup>-1</sup> in an IRMPD spectrum measured with a 3 s

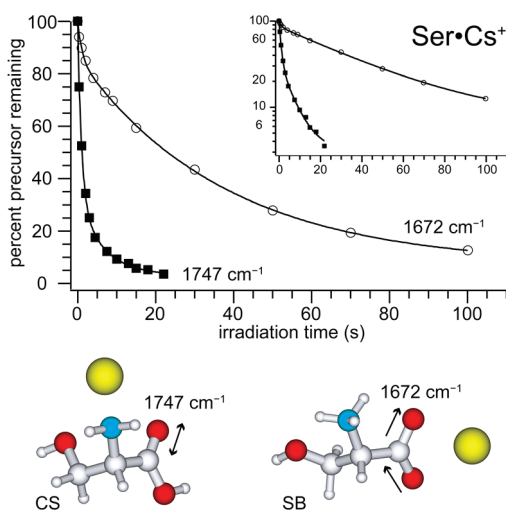


**Figure 4.** IRMPD kinetics for Ser·Cs<sup>+</sup> at 1747 (filled squares) and 1672 cm<sup>-1</sup> (open circles) with biexponential fits (lines). The same data with a logarithmic y-axis are inset to make the biexponential kinetic behavior clearer. Arrows in representative CS and SB structures indicate the vibrational modes excited at the photon energies used.

irradiation time would have a relative intensity that is artificially 8.8 (14/1.6) times too large!

With ions for which the lowest-energy structure has a high barrier to dissociation, signature bands indicating the presence of this lowest-energy structure may not be measurable at irradiation times on the order of the induction period, even though dissociation of higher-energy structures with lower dissociation barriers at other photon energies is observed. This could lead to the erroneous conclusion that this lowest-energy structure is not present, when in fact it is an artifact of how these data are typically acquired. Because induction periods should be longer on the tails of a spectral peak, improper treatment of induction periods can also result in misleading apparent linewidths. These results indicate that measuring IRMPD kinetics out to irradiation times where extensive depletion of the precursor occurs can be very useful in removing such potential ambiguities.

**Complementary Resonance Analysis: Ser·Cs<sup>+</sup> and Arg·Na<sup>+</sup>.** Previous IRMPD spectroscopy experiments by Armentrout and co-workers indicate that Ser·Cs<sup>+</sup> adopts a mixture of CS and SB isomers at 298 K.<sup>28</sup> These two populations are distinguished spectroscopically by the presence of a carboxylic acid carbonyl stretch at 1747 cm<sup>-1</sup> for the CS isomer family and a carboxylate antisymmetric stretch at 1672 cm<sup>-1</sup> for the SB isomer family. In the reported IRMPD spectrum of this ion, the band at 1747 cm<sup>-1</sup> is much more intense than that at 1672 cm<sup>-1</sup>, and it was concluded that the CS isomer family makes up most of the ion population.<sup>28</sup> IRMPD kinetics of this ion at these two photon energies are shown in Figure 4. Biexponential kinetics at both photon energies with no induction period are observed. Fits to these data indicate that about ~3–7% of the ion population cannot be dissociated on the time-scale of these experiments. Interestingly, the fast rate constants associated with the resonant populations at these two photon energies are nearly identical, and an IRMPD spectrum that takes into account the nonlinear kinetics observed here would have spectral bands of nearly equal intensity at these two frequencies, rather than the disparate intensities previously reported using a single irradiation time.<sup>28</sup>

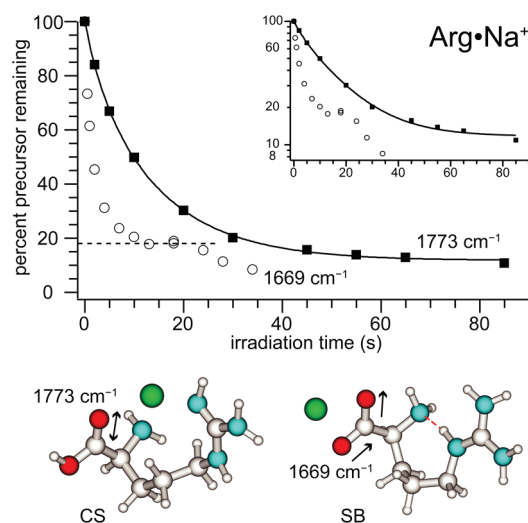


**Figure 5.** IRMPD kinetics for Arg·Na<sup>+</sup> at 1669 (open circles) and 1773 cm<sup>-1</sup> (filled squares) with dashed line indicating the y-value of the inflection point for the 1669 cm<sup>-1</sup> data and solid line indicating a biexponential fit for the 1773 cm<sup>-1</sup> data. The same data with a logarithmic y-axis are inset to make the inflection point and biexponential kinetic behavior clearer. Arrows in representative CS and SB structures indicate the vibrational modes excited at the photon energies used.

Taking the nondissociable population into account, the 1747 cm<sup>-1</sup> data indicate that ~64–75% of the dissociable ion population comprises CS isomers (fast rate constant = ~1.0 s<sup>-1</sup>) and the remaining ~25–36% are SB isomers (slow rate constant = ~0.1 s<sup>-1</sup>). Fits to the 1672 cm<sup>-1</sup> data are also consistent with a slightly larger CS population, indicating ~15–21% of the dissociable ions are SB isomers (fast rate constant = ~0.9 s<sup>-1</sup>) and ~79–85% are CS isomers (slow rate constant = ~0.03 s<sup>-1</sup>). The small difference in the fitted populations obtained at these two photon energies is likely a result of the significant overlap of the two spectral bands or uncertainty of fitting double exponential kinetics that have experimental noise,<sup>42</sup> but it is clear that CS isomers make up the majority (~64–85%) of the ion population. If the initial ion population represent as Boltzmann distribution and kinetic trapping has not occurred, these isomer populations correspond to a Gibbs free energy difference of ~1.4–4.3 kJ/mol between the CS and SB isomers at 298 K, a much smaller difference than those previously reported based on theoretical computations.<sup>28</sup> This energy range is remarkably narrow and serves as a stringent benchmark for theory.

A similar complementary resonance analysis was performed for Arg·Na<sup>+</sup>, which was previously reported to consist of ~90% SB structures and ~10% CS structures based on IRMPD spectroscopy experiments with a fixed irradiation time.<sup>5</sup> Here, the ions were irradiated at the carboxylate antisymmetric stretch (1669 cm<sup>-1</sup>), resonant with SB structures, or the carboxylic acid carbonyl stretch (1773 cm<sup>-1</sup>), resonant with CS structures.<sup>26</sup> The resulting IRMPD kinetics are shown in Figure 5. Similar to that for ArgGly·Na<sup>+</sup> (vide supra), there is an inflection point at ~15 s irradiation time in the 1669 cm<sup>-1</sup> kinetics that indicates interconversion of the CS population to SB isomers occurs on a time scale much slower than resonant photodissociation of the initial SB population. This inflection point corresponds to ~82% depletion of the initial ion population corresponding to the SB isomer. Irradiation at 1733 cm<sup>-1</sup> results in slower photodissociation

kinetics, and  $\sim 11\%$  of the ion population is not depleted on the time scale of these experiments. Biexponential fitting of the  $1733\text{ cm}^{-1}$  data indicates that  $\sim 7\text{--}24\%$  of the ion population are CS structures and  $\sim 76\text{--}93\%$  are SB structures when the  $\sim 11\%$  nondissociable population is taken into account. These results are in good agreement with the complementary data at  $1669\text{ cm}^{-1}$ . For an initial ion population that is thermal, these relative populations indicate that the Gibbs free energy of the SB isomer is  $\sim 2.9\text{--}6.4\text{ kJ/mol}$  lower than that of the CS isomers at  $298\text{ K}$ .

## CONCLUSIONS

IRMPD kinetics of ions with one or more isomer populations were measured using radiation from a free electron laser (FELIX). For ions with just one isomer (anilinium and benzoate), first-order, monoexponential kinetics were observed to  $\sim 93\%$  depletion of the initial ion population, indicating that as much as  $\sim 7\%$  of the trapped ions in all these experiments can have poor overlap with the laser beam. For ions with two spectroscopically distinguishable isomer populations, three forms of IRMPD kinetic behaviors were observed when the ions were irradiated at photon energies resonant with only one isomer population: (1) depletion of the ion population up to an inflection point, indicating slow interconversion of the off-resonant isomer to a resonant isomer, (2) monoexponential kinetics indicative of rapid isomer interconversion, with or without a slow-heating induction period, or (3) biexponential kinetics indicative of isomer interconversion without a significant induction period. For cases 1 and 3, isomer populations and, hence, relative Gibbs free energies can be readily obtained, as for  $\text{ArgGly}\cdot\text{Na}^+$  and  $\text{Arg}\cdot\text{Na}^+$ , where complementary resonance experiments were performed that yielded consistent isomer populations and remarkably narrow ranges for relative Gibbs free energies. For  $\text{ArgGly}\cdot\text{Li}^+$ , which exhibited type 2 behavior in these experiments, relative ion populations could not be obtained, because the interconversion barrier for the two isomer families of this ion is relatively low.

These results illustrate the advantage of combining IRMPD kinetics measured at select photon energies with IRMPD spectroscopy for measuring isomer populations. Evidence for kinetic trapping of high-energy structures of some ions generated from electrospray has been reported.<sup>21,22</sup> Although a high isomerization barrier observed for some of the ions here is necessary for kinetic trapping, the presence of a high isomerization barrier by itself does not necessarily indicate kinetic trapping has occurred, because annealing into a thermal distribution can occur. Evidence for kinetic trapping can be obtained by measuring spectra and kinetics of ions formed from different electrospray solvents or by varying electrospray source conditions. For thermal ion populations, the relative energies of isomers obtained from IRMPD kinetic data serve as a stringent benchmark for theory. Also elucidated in these experiments are some dangers of interpreting IRMPD (or, indeed, IRPD) spectra measured at just a single irradiation time, because IR(M)PD can often include significant induction periods or kinetics that are not monoexponential, in which case relative IR(M)PD spectra and band linewidths derived from single irradiation times may vary with the choice of irradiation time and could even lead to the erroneous conclusion that a slow-heating, lowest-energy isomer population is not present.

In IR(M)PD kinetics experiments, deviations from first-order, monoexponential kinetics are often apparent only after a

significant fraction, sometimes  $\sim 80\text{--}90\%$ , of the initial precursor ion population has been dissociated. Overlap of as much of the ion population as possible with the laser beam is therefore necessary to obtain a high degree of precision in population analyses. Although  $>96\%$  overlap has been previously demonstrated with an on-axis ion irradiation geometry,<sup>34,35</sup> and  $\sim 93\%$  overlap is achieved in these experiments in which an off-axis multipass ion irradiation geometry is used,<sup>1</sup> it would be highly advantageous in future instrument designs to achieve a yet greater extent of overlap between the laser beam and ion cloud, within the competing constraints of ion space-charge limits and high laser fluence necessary to dissociate stable ions.

## AUTHOR INFORMATION

### Corresponding Author

\*Fax: (510) 642-7714. E-mail: williams@cchem.berkeley.edu.

## ACKNOWLEDGMENT

The authors thank Dr. Britta Redlich and the FELIX support staff for excellent hospitality as well as the National Science Foundation (Grants CHE-1012833 and OISE-730072) for generous financial support.

## REFERENCES

- (1) Eyler, J. R. *Mass Spectrom. Rev.* **2009**, *28*, 448-467.
- (2) Polfer, N. C.; Oomens, J. *Mass Spectrom. Rev.* **2009**, *28*, 468-494.
- (3) Ayotte, P.; Bailey, C. G.; Kim, J.; Johnson, M. A. *J. Chem. Phys.* **1998**, *108*, 444-449.
- (4) Bakker, J. M.; Besson, T.; Lemaire, J.; Scuderi, D.; Maitre, P. *J. Phys. Chem. A* **2007**, *111*, 13415-13424.
- (5) Bush, M. F.; O'Brien, J. T.; Prell, J. S.; Saykally, R. J.; Williams, E. R. *J. Am. Chem. Soc.* **2007**, *129*, 1612-1622.
- (6) Dryza, V.; Poad, B. L. J.; Bieske, E. J. *J. Phys. Chem. A* **2009**, *113*, 6044-6048.
- (7) Gregoire, G.; Velasquez, J.; Duncan, M. A. *Chem. Phys. Lett.* **2001**, *349*, 451-457.
- (8) Kamariotis, A.; Boyarkin, O. V.; Mercier, S. R.; Beck, R. D.; Bush, M. F.; Williams, E. R.; Rizzo, T. R. *J. Am. Chem. Soc.* **2006**, *128*, 905-916.
- (9) Macleod, N. A.; Simons, J. P. *Phys. Chem. Chem. Phys.* **2004**, *6*, 2821-2826.
- (10) Mahjoub, A.; Chakraborty, A.; Lepere, V.; Le Barbu-Debus, K.; Guchhait, N.; Zehnacker, A. *Phys. Chem. Chem. Phys.* **2009**, *11*, S160-S169.
- (11) Oh, H. B.; Lin, C.; Hwang, H. Y.; Zhai, H. L.; Breuker, K.; Zabrouskov, V.; Carpenter, B. K.; McLafferty, F. W. *J. Am. Chem. Soc.* **2005**, *127*, 4076-4083.
- (12) Okumura, M.; Yeh, L. I.; Lee, Y. T. *J. Chem. Phys.* **1988**, *88*, 79-91.
- (13) Pribble, R. N.; Zwier, T. S. *Faraday Discuss.* **1994**, *97*, 229-241.
- (14) Roscioli, J. R.; Hammer, N. I.; Johnson, M. A. *J. Phys. Chem. A* **2006**, *110*, 7517-7520.
- (15) Sawamura, T.; Fujii, A.; Sato, S.; Ebata, T.; Mikami, N. *J. Phys. Chem.* **1996**, *100*, 8131-8138.
- (16) Stearns, J. A.; Das, A.; Zwier, T. S. *Phys. Chem. Chem. Phys.* **2004**, *6*, 2605-2610.
- (17) Wang, Y. S.; Tsai, C. H.; Lee, Y. T.; Chang, H. C.; Jiang, J. C.; Asvany, O.; Schlemmer, S.; Gerlich, D. *J. Phys. Chem. A* **2003**, *107*, 4217-4225.
- (18) Lemaire, J.; Boissel, P.; Heninger, M.; Mauclair, G.; Bellec, G.; Mestdagh, H.; Simon, A.; Caer, S. L.; Ortega, J. M.; Glotin, F.; Maitre, P. *Phys. Rev. Lett.* **2002**, *89*, 4.
- (19) Valle, J. J.; Eyler, J. R.; Oomens, J.; Moore, D. T.; van der Meer, A. F. G.; von Helden, G.; Meijer, G.; Hendrickson, C. L.; Marshall, A. G.; Blakney, G. T. *Rev. Sci. Instrum.* **2005**, *76*, 023103.

- (20) Prell, J. S.; O'Brien, J. T.; Williams, E. R. *J. Am. Soc. Mass Spectrom.* **2010**, *21*, 800–809.
- (21) Steill, J. D.; Oomens, J. *J. Am. Chem. Soc.* **2009**, *131*, 13570–13571.
- (22) Tian, Z. X.; Kass, S. R. *J. Am. Chem. Soc.* **2008**, *130*, 10842–10843.
- (23) Gross, D. S.; Zhao, Y. X.; Williams, E. R. *J. Am. Soc. Mass Spectrom.* **1997**, *8*, 519–524.
- (24) Pierson, N. A.; Valentine, S. J.; Clemmer, D. E. *J. Phys. Chem. B* **2010**, *114*, 7777–7783.
- (25) Ruotolo, B. T.; Robinson, C. V. *Curr. Opin. Chem. Biol.* **2006**, *10*, 402–408.
- (26) Forbes, M. W.; Bush, M. F.; Polfer, N. C.; Oomens, J.; Dunbar, R. C.; Williams, E. R.; Jockusch, R. A. *J. Phys. Chem. A* **2007**, *111*, 11759–11770.
- (27) Prell, J. S.; Demireva, M.; Williams, E. R. *J. Am. Chem. Soc.* **2009**, *131*, 1232–1242.
- (28) Armentrout, P. B.; Rodgers, M. T.; Oomens, J.; Steill, J. D. *J. Phys. Chem. A* **2008**, *112*, 2248–2257.
- (29) Dunbar, R. C.; Steill, J. D.; Polfer, N. C.; Oomens, J. *J. Phys. Chem. B* **2009**, *113*, 10552–10554.
- (30) Kupser, P.; Steill, J. D.; Oomens, J.; Meijer, G.; von Helden, G. *Phys. Chem. Chem. Phys.* **2008**, *10*, 6862–6866.
- (31) O'Brien, J. T.; Williams, E. R. *J. Phys. Chem. A* **2008**, *112*, 5893–5901.
- (32) Polfer, N. C.; Paizs, B.; Snoek, L. C.; Compagnon, I.; Suhai, S.; Meijer, G.; von Helden, G.; Oomens, J. *J. Am. Chem. Soc.* **2005**, *127*, 8571–8579.
- (33) Prell, J. S.; O'Brien, J. T.; Steill, J. D.; Oomens, J.; Williams, E. R. *J. Am. Chem. Soc.* **2009**, *131*, 11442–11449.
- (34) Prell, J. S.; Chang, T. M.; O'Brien, J. T.; Williams, E. R. *J. Am. Chem. Soc.* **2010**, *132*, 7811–7819.
- (35) Prell, J. S.; Corraera, T. C.; Chang, T. M.; Biles, J. A.; Williams, E. R. *J. Am. Chem. Soc.* **2010**, *132*, 14733–14735.
- (36) Elliott, B. M.; Relph, R. A.; Roscioli, J. R.; Bopp, J. C.; Gardenier, G. H.; Guasco, T. L.; Johnson, M. A. *J. Chem. Phys.* **2008**, *129*, 094303.
- (37) Relph, R. A.; Guasco, T. L.; Elliott, B. M.; Kamrath, M. Z.; McCoy, A. B.; Steele, R. P.; Schofield, D. P.; Jordan, K. D.; Viggiano, A. A.; Ferguson, E. E.; Johnson, M. A. *Science* **2010**, *327*, 308–312.
- (38) Clarkson, J. R.; Dian, B. C.; Moriggi, L.; DeFusco, A.; McCarthy, V.; Jordan, K. D.; Zwier, T. S. *J. Chem. Phys.* **2005**, *122*, 214311.
- (39) Pillsbury, N. R.; Zwier, T. S. *J. Phys. Chem. A* **2009**, *113*, 126–134.
- (40) Nagornova, N. S.; Rizzo, T. R.; Boyarkin, O. V. *J. Am. Chem. Soc.* **2010**, *132*, 4040–4041.
- (41) Stearns, J. A.; Seaiby, C.; Boyarkin, O. V.; Rizzo, T. R. *Phys. Chem. Chem. Phys.* **2009**, *11*, 125–132.
- (42) Schnier, P. D.; Williams, E. R. *Anal. Chem.* **1998**, *70*, 3033–3041.
- (43) Polfer, N. C.; Oomens, J.; Moore, D. T.; von Helden, G.; Meijer, G.; Dunbar, R. C. *J. Am. Chem. Soc.* **2006**, *128*, 517–525.
- (44) Data retrieved from <http://webbook.nist.gov>.
- (45) Freitas, M. A.; Hendrickson, C. L.; Marshall, A. G. *J. Am. Chem. Soc.* **2000**, *122*, 7768–7775.
- (46) Jockusch, R. A.; Paech, K.; Williams, E. R. *J. Phys. Chem. A* **2000**, *104*, 3188–3196.
- (47) MacAleese, L.; Maitre, P. *Mass Spectrom. Rev.* **2007**, *26*, 583–605.
- (48) Prell, J. S.; Flick, T. G.; Oomens, J.; Berden, G.; Williams, E. R. *J. Phys. Chem. A* **2010**, *114*, 854–860.
- (49) Shin, J. W.; Hammer, N. I.; Diken, E. G.; Johnson, M. A.; Walters, R. S.; Jaeger, T. D.; Duncan, M. A.; Christie, R. A.; Jordan, K. D. *Science* **2004**, *304*, 1137–1140.
- (50) Bush, M. F.; Saykally, R. J.; Williams, E. R. *J. Am. Chem. Soc.* **2007**, *129*, 2220–2221.
- (51) Ayotte, P.; Kelley, J. A.; Nielsen, S. B.; Johnson, M. A. *Chem. Phys. Lett.* **2000**, *316*, 455–459.
- (52) Grégoire, G.; Gageot, M. P.; Marinica, D. C.; Lemaire, J.; Schermann, J. P.; Desfrancois, C. *Phys. Chem. Chem. Phys.* **2007**, *9*, 3082–3097.
- (53) Heaton, A. L.; Bowman, V. N.; Oomens, J.; Steill, J. D.; Armentrout, P. B. *J. Phys. Chem. A* **2009**, *113*, 5519–5530.
- (54) Kapota, C.; Lemaire, J.; Maitre, P.; Ohanessian, G. *J. Am. Chem. Soc.* **2004**, *126*, 1836–1842.
- (55) Miller, D. J.; Lisy, J. M. *J. Am. Chem. Soc.* **2008**, *130*, 15393–15404.
- (56) Nicely, A. L.; Miller, D. J.; Lisy, J. M. *J. Am. Chem. Soc.* **2009**, *131*, 6314–6315.
- (57) O'Brien, J. T.; Prell, J. S.; Bush, M. F.; Williams, E. R. *J. Am. Chem. Soc.* **2010**, *132*, 8248–8249.
- (58) Pribble, R. N.; Zwier, T. S. *Science* **1994**, *265*, 75–79.
- (59) Drayss, M. K.; Blunk, D.; Oomens, J.; Gao, B.; Wyttenbach, T.; Bowers, M. T.; Schäfer, M. *J. Phys. Chem. A* **2009**, *113*, 9543–9550.
- (60) Drayss, M. K.; Blunk, D.; Oomens, J.; Schäfer, M. *J. Phys. Chem. A* **2008**, *112*, 11972–11974.
- (61) Vaden, T. D.; de Boer, T. S. J. A.; Simons, J. P.; Snoek, L. C.; Suhai, S.; Paizs, B. *J. Phys. Chem. A* **2008**, *112*, 4608–4616.
- (62) Walters, R. S.; Pillai, E. D.; Duncan, M. A. *J. Am. Chem. Soc.* **2005**, *127*, 16599–16610.
- (63) Wu, R. H.; McMahon, T. B. *J. Am. Chem. Soc.* **2007**, *129*, 4864–4865.
- (64) Wu, R. H.; McMahon, T. B. *Angew. Chem., Int. Ed.* **2007**, *46*, 3668–3671.
- (65) Zhou, J.; Santambrogio, G.; Brummer, M.; Moore, D. T.; Meijer, G.; Neumark, D. M.; Asmis, K. R. *J. Chem. Phys.* **2006**, *125*, 111102.